



Universiteit
Leiden
The Netherlands

Development of the first potential nonpeptidic positron emission tomography tracer for the imaging of CCR2 receptors

Wagner, S.; Moura Gatti, F.; Silva, D.G. de; Ortiz Zacarias, N.V.; Zweemer, A.J.M.; Hermann, S.; ... ; Junker, A.

Citation

Wagner, S., Moura Gatti, F., Silva, D. G. de, Ortiz Zacarias, N. V., Zweemer, A. J. M., Hermann, S., ... Junker, A. (2020). Development of the first potential nonpeptidic positron emission tomography tracer for the imaging of CCR2 receptors. *Chemmedchem*, 16(4), 640-645. doi:10.1002/cmdc.202000728

Version: Publisher's Version

License: [Creative Commons CC BY-NC-ND 4.0 license](https://creativecommons.org/licenses/by-nc-nd/4.0/)

Downloaded from: <https://hdl.handle.net/1887/3134856>

Note: To cite this publication please use the final published version (if applicable).


 Very Important Paper

Development of the First Potential Nonpeptidic Positron Emission Tomography Tracer for the Imaging of CCR2 Receptors

Stefan Wagner^{+, [a]} Fernando de Moura Gatti^{+, [b, i]} Daniel G. Silva,^[c] Natalia V. Ortiz Zacarias,^[d] Annelien J. M. Zweemer,^[d] Sven Hermann,^[c] Monica De Maria,^[e] Michael Koch,^[f] Christina Weiss,^[f] Dirk Schepmann,^[b] Laura H. Heitman,^[d] Nuska Tschammer,^[g] Klaus Kopka,^[h] and Anna Junker^{*[b, c]}

Herein we report the design and synthesis of a series of highly selective CCR2 antagonists as ¹⁸F-labeled PET tracers. The derivatives were evaluated extensively for their off-target profile at 48 different targets. The most potent and selective candidate

was applied *in vivo* in a biodistribution study, demonstrating a promising profile for further preclinical development. This compound represents the first potential nonpeptidic PET tracer for the imaging of CCR2 receptors.

Introduction

The C–C chemokine receptor type 2 (CCR2) is a key player in the trafficking of lymphocytes and monocytes/macrophages leading to the development of various pathophysiological processes like inflammatory and autoimmune diseases,^[1] tumor growth and metastasis formation.^[2] CCR2 receptor is increasingly gaining attention in the field of positron emission tomography (PET) imaging as a promising diagnostic target for lung inflammation,^[3] injured heart^[4] or pancreatic ductal adenocarcinoma (phase 1; NCT03851237, 1R01CA235672-01, 201807099). So far only a peptidic ligand that binds to the first extracellular loop of the CCR2 receptor ECL1i was applied in PET imaging either as ⁶⁴Cu-DOTA-ECL1i or ⁶⁸Ga-DOTA-ECL1i

conjugate.^[3–4] There are no small-molecule, nonpeptidic PET tracers for the imaging of CCR2 receptors reported thus far.

The CCR2 receptors share 71% sequence identity and an overlapping expression pattern with the C–C chemokine type 5 (CCR5) receptors.^[5] The CCR5 receptor is expressed on a variety of cells and tissues such as monocytes, macrophages, T-lymphocytes, microglia, dendritic cells, the endothelium, and vascular smooth muscle. The CCR2 expression is more restricted to certain cell types such as monocytes, NK (natural killer) cells, and T lymphocytes.^[6] Many potent CCR2 ligands demonstrate affinity to both receptors.^[7] In the past, we have reported the design and synthesis of novel, selective as well as dual-targeting CCR2 and CCR5 receptor antagonists,^[8] as well as the positive allosteric modulators (PAMs) for the CCR5 receptors.^[9] Based on

[a] Dr. S. Wagner⁺

Department of Nuclear Medicine
University Hospital Münster
Albert-Schweitzer-Campus 1, Building A1
48149 Münster (Germany)

[b] Dr. F. de Moura Gatti,⁺ Dr. D. Schepmann, Dr. A. Junker
Institut für Pharmazeutische und Medizinische Chemie der Universität
Münster

Corrensstraße 48, 48149 Münster (Germany)

[c] Dr. D. G. Silva, Dr. S. Hermann, Dr. A. Junker
European Institute for Molecular Imaging (EIMI)
Waldeyerstraße 15, 48149 Münster (Germany)
E-mail: anna.junker@wwu.de

[d] Dr. N. V. Ortiz Zacarias, Dr. A. J. M. Zweemer, Prof. Dr. L. H. Heitman
Leiden Academic Centre for Drug Research (LACDR)
Leiden University
Einsteinweg 55, 2333 CC Leiden (The Netherlands)

[e] M. De Maria
Department of Developmental Biology
Friedrich Alexander University
Staudtstraße 5, 91058 Erlangen (Germany)

[f] Dr. M. Koch, C. Weiss
Bayer AG, Research & Development
Lead Discovery Wuppertal
Aprather Weg 18a, Gebäude 456
42096 Wuppertal (Germany)

[g] Dr. N. Tschammer


Department of Chemistry and Pharmacy
Emil Fischer Center
Friedrich Alexander University Erlangen–Nürnberg
Schuhstraße 19, 91052 Erlangen (Germany)


[h] Prof. Dr. K. Kopka
Helmholtz-Zentrum Dresden-Rossendorf
Institut für Radiopharmazeutische Krebsforschung
Bautzner Landstraße 400
01328 Dresden (Germany)

and
Faculty of Chemistry and Food Chemistry
Technische Universität Dresden
01062 Dresden (Germany)

[i] Dr. F. de Moura Gatti⁺
Faculdade de Ciências Farmacêuticas
Universidade de São Paulo
Av. Prof. Lineu Prestes, 580
CEP 05508-900, São Paulo, SP (Brazil)

[*] These authors contributed equally to this work.

 Supporting information for this article is available on the WWW under <https://doi.org/10.1002/cmdc.202000728>

 © 2020 The Authors. ChemMedChem published by Wiley-VCH GmbH. This is an open access article under the terms of the Creative Commons Attribution Non-Commercial NoDerivs License, which permits use and distribution in any medium, provided the original work is properly cited, the use is non-commercial and no modifications or adaptations are made.

this work we envisaged to evaluate fluorine-18 radiolabeled CCR2 targeting ligands as PET radiotracers for molecular imaging of inflammation and cancer.

Our previous structure–activity and structure–affinity studies of novel CCR2 and CCR5 receptors targeting compounds derived from TAK-779 (1) revealed a first strategy for the introduction of high CCR2 receptor selectivity. While TAK-779 (1) is more or less equipotent at CCR2 and CCR5 receptors introduction of a bulky isopropoxy residue at the 6-position of a pyridine ring as seen in compound 2 (Figure 1) yielded different properties of binding to the active site residues within the CCR2 and CCR5 receptors, leading to higher CCR2 selectivity (Table 1, IC_{50} ($[^{125}I]$ CCL2) = 19 nM vs. IC_{50} ($[^3H]$ TAK-779) = 468 nM). Other pyridine derivatives were inactive.^[8a]

Results and Discussion

Following the idea of addressing different electrostatic properties by the isopropoxy derivative 2, a series of CCR2 selective antagonists 6a–c bearing a flexible ω -fluoroalkoxy side chain was developed. The phenol derivative 3 served as a starting structure for the introduction of the alkoxy side chain. As the influence of the chain length on the CCR2 and CCR5 receptor activity/affinity should be examined, propyloxy (4a, $n=3$),

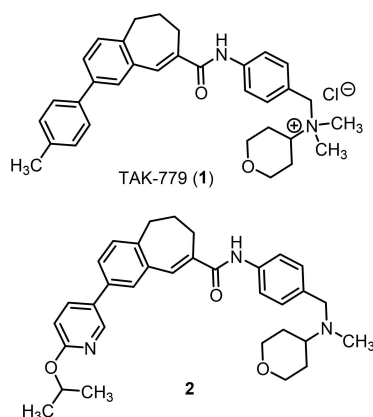
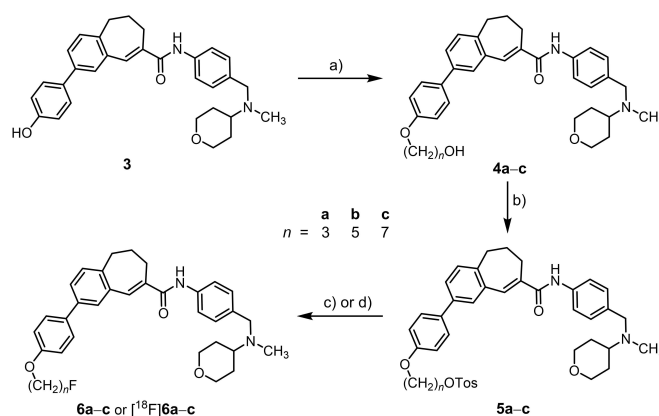


Figure 1. TAK-779 (1) and compound 2.



Scheme 1. Synthesis of ω -fluoroalkyl derivatives 6a–c. a) ω -bromoalkanol-1-ol (1.1 equiv.), K_2CO_3 (2 equiv.), DMF, 60 °C, 12 h, 70–84%; b) DMAP (0.25 equiv.), Et_3N (4.65 equiv.), 4-toluenesulfonyl chloride (2 equiv.), –25 °C (0.5 h), then RT, 20 h, 74–90%; c) Bu_4NF (1 M in THF, 20 equiv.), THF, RT, 12 h, 73–84%; d) $K(K_{2,2,2})[^{18}F]F$, K_2CO_3 , DMSO, 100 °C, 20 min.

pentyloxy (4b, $n=5$) and heptyloxy (4a, $n=7$) side chains were considered. The high acidity of the phenol 3 allows deprotonation with weak bases without affecting the primary alcohol of the ω -halogenalkanols used. The reactivity of the ω -halogenalkanols is dependent on the halogen leaving group ($I > Br > Cl$). However, the reaction with 3-iodopropan-1-ol led to dialkylation of 3 (second alkyl group attached to the tertiary amine). Because we assumed that the dialkylation was due to the high reactivity of 3-iodopropan-1-ol, 3-bromopropan-1-ol with reduced reactivity was employed. Reaction of 3 with 3-bromopropan-1-ol and K_2CO_3 in DMF afforded selectively 4a in 84% yield. The homologous alcohols 4b and 4c were prepared analogously by alkylation of phenol 3 with 5-bromopentan-1-ol and 7-bromoheptan-1-ol, respectively (Scheme 1). The compounds 5a–c served as precursors for the development of fluorinated PET ligands $[^{18}F]6a-c$. The introduction of an ^{18}F -atom into the molecule requires a good leaving group. Therefore, the primary alcohols 4a–c were converted into the tosylates 5a–c. The reaction of the alcohols 4a–c with tosyl chloride and 4-dimethylaminopyridine (DMAP, *Steglich* catalyst) provided the tosylates 5a–c.⁹ The *in vitro* receptor activities and affinities of the ^{18}F -labeled PET tracers cannot be recorded

Table 1. CCR2 and CCR5 activities and affinities of TAK-779 (1), the reference compound 2, the alcohols 3, 4a–c and fluorinated ligands 6a–c.

Cmpd.	CCR2 $IC_{50} \pm SEM$ [nM]		Ca^{2+} flux, hCCR2	β -Arrestin, mCCR2	CCR5			
	$[^{125}I]$ CCL2	$[^3H]$ INCB			$[^3H]$ TAK-779 $IC_{50} \pm SEM$ [nM]	β Arrestin, hCCR5, CCL5-mediated K_b [nM]	cAMP BRET, CCL5-mediated K_b [nM]	cAMP BRET, CCL4-mediated K_b [nM]
TAK-779 (1)	$2.0 \pm 0.7^{[a]}$	$50 \pm 5^{[a]}$	$0.95^{[a]}$	$23^{[a]}$	8.8 ± 1.7^a	12 ± 1.2	65.5	7.5
2	$19 \pm 4.2^{[a]}$	–	$2.7^{[a]}$	$90^{[a]}$	468 ^a	–	–	–
3	$35\%^{[b]}$	–	82	1360	1500	–	–	–
4a	199	$51\%^{[b]}$	45	783	970	–	–	–
4b	326	$53\%^{[b]}$	10	117	3100	–	–	–
4c	83	$56\%^{[b]}$	1.1	54	2300	–	–	–
6a	$48\%^{[b]}$	118 ± 20	130	1110	2700	684 ± 219	2300	551
6b	14 ± 7	609 ± 188	0.76	40	2000	529 ± 142	580	65.4
6c	93 ± 8	494 ± 38	1.1	17	3600	378 ± 114	288	27.1

All experiments were performed in at least triplicate ($n=3$). [a] See ref. [8a]. [b] % inhibition at a test compound concentration of 1 μ M.

directly with the radiolabeled ligands due to the small amount and the short physical half-life of the labeled compounds. Therefore, the *in vitro* activities and affinities to the CCR2 and other receptors/targets were determined using the non-radioactive ^{19}F -labeled analogues. The synthesis of the non-radioactive ^{19}F counterparts **6a–c** can be performed by direct fluorination of the alcohols **4a–c** or by the introduction of an appropriate leaving group and subsequent $\text{S}_{\text{N}}2$ substitution. Tetrabutylammonium fluoride (TBAF) is a common fluorinating reagent. The bulky tetraalkylammonium counterion reduces the ionic bond strength and generates a “naked” fluoride ion with a good solubility in organic solvents.^[10] As the tosylates **5a–c** were already prepared for the radiolabeling reaction, they were also employed for the fluorination with TBAF. Tosylates **5a–c** were reacted with TBAF in THF, which afforded the pure fluoro derivatives **6a–c** in 73–84% yield (Scheme 1).

The compounds were evaluated for their *in vitro* CCR2 activities and affinities as well as their selectivity towards CCR5 receptors in functional as well as in binding assays. The hydroxyalkoxy derivatives **4a–c** display very low CCR2 and CCR5 receptor affinities and moderate to high CCR2 receptor potencies (Table 1). The heptyloxy derivative with a primary alcohol at the end (**4c**) shows the highest CCR2 affinity/activity ($\text{IC}_{50}([\text{}^{125}\text{I}]\text{CCL2}) = 83 \text{ nM}$, $\text{IC}_{50}(\text{Ca}^{2+}\text{-flux, hCCR2}) = 1.1 \text{ nM}$, $\text{IC}_{50}(\beta\text{-arrestin, mCCR2}) = 54 \text{ nM}$).

However, the fluoroalkoxy derivatives **6a–c** do not follow the same trend in their SAR. The pentyloxy compound **6b** displays the highest CCR2 binding in the $[\text{}^{125}\text{I}]\text{CCL2}$ assay with an IC_{50} -value of 14 nM and the highest CCR2 activity in the Ca^{2+} -flux assay using the human CCR2 receptor, indicating an IC_{50} -value of 0.76 nM. Furthermore, **6b** is highly selective against CCR5 receptors ($\text{IC}_{50}(\text{CCR5}; [\text{}^3\text{H}]\text{TAK-779}) = 2000 \text{ nM}$). The fluoroalkoxy derivatives **6a–c** show a probe-dependent CCR5 activity when compared to TAK-779; whereas TAK-779 (1) binding affects CCL5- as well as CCL4-dependent CCR5 receptor activity. The fluoroalkoxy derivatives **6b** and **6c** display only high activity in the cAMP-BRET CCL4-mediated assay with K_{b} values of 65.4 and 27.1 nM, respectively. Only moderate activity is seen in β -arrestin and cAMP BRET CCL5-mediated CCR5 assays, indicating a different binding mode at the CCR5 receptors as compared with that of TAK-779 (1).

Moreover, the fluoroalkoxy derivatives **6a–c** were screened in the in-house σ_1 , σ_2 assays and in a panel of 45 different targets (hERG, 5-HT_{1A}, 5-HT_{1B}, 5-HT_{1D}, 5-HT_{1E}, 5-HT_{2A}, 5-HT_{2B}, 5-HT_{2C}, 5-HT₃, 5-HT_{5A}, 5-HT₆, 5-HT₇, D₁₋₅, SERT, NET, DAT, MOR, KOR, DOR, GABA_A, H₁₋₄, α_{1A} , α_{1B} , α_{2A} , α_{2B} , α_{2C} , α_{1D} , β_{1-3} , M₁₋₅, BZP Rat brain site, PBR) within the NIMH Psychoactive Drug Screen-

Table 3. Results of the radiosynthesis of compounds $[\text{}^{18}\text{F}]\text{6a–c}$.

Cmpd.	Synthesis time [min]	A_{m} [GBq/ μmol]	RCY [%] (decay-corrected)
$[\text{}^{18}\text{F}]\text{6a}$	94 ± 13	4–70	40 ± 3 ^[a]
$[\text{}^{18}\text{F}]\text{6b}$	113 ± 27	3–31	28 ± 5 ^[b]
$[\text{}^{18}\text{F}]\text{6c}$	91 ± 10	5–54	25 ± 6 ^[c]

[a] $n = 5$, [b] $n = 9$, [c] $n = 6$.

ing Program for their off-target affinity/activity. In Table 2, the data for detectable ($< 10 \mu\text{M}$) off-target affinity/activity of compounds **6a–c** is given. Hereby, the fluoropentoxy derivative **6b** displayed the highest selectivity profile within the series. Compound **6b** showed moderate affinity in the radioligand binding assays for σ_1 ($K_{\text{i}}([\text{}^3\text{H}]\text{-}(+)\text{-pentazocine}) = 0.32 \mu\text{M}$) and very low affinity to $\alpha_{2\text{B}}$ receptors ($K_{\text{i}}([\text{}^3\text{H}]\text{Rauwolscine}) = 6.81 \mu\text{M}$). The inhibition of the hERG channel (Kv_{11.1} potassium ion channel, KCNH2) is widely regarded as the predominant cause of drug-induced QT prolongation. The moderate hERG activity and, therefore, potential cardiotoxicity of compound **6b** of 1.72 μM in the FluxOR assay would represent a considerable limitation to a drug development program. However, diagnostic PET tracers are applied in extremely low concentrations; therefore, not reaching the effective concentration required for cardiotoxicity. Taken together, the fluoropentoxy derivative **6b** displayed high CCR2 affinity/activity combined with a favorable off-target selectivity profile and was therefore chosen as a promising candidate for *in vivo* evaluation as a potential PET tracer.

PET measurements can be performed with different radio-nuclides such as ^{11}C , ^{13}N , ^{15}O and ^{18}F . ^{13}N and ^{15}O are very limited due to their short physical half-life ($< 10 \text{ min}$) and are mostly used for the imaging of perfusion processes.^[11] $[\text{}^{18}\text{F}]\text{fluoride}$ offers several advantages over $[\text{}^{11}\text{C}]\text{carbon}$, such as longer physical half-life (110 vs. 20 min), maximal β^+ -particle energy of 650 keV vs. 960 keV, and higher quality images with higher spatial resolution in PET measurements.^[11–12] In our efforts to develop an ^{18}F -labeled CCR2 receptor PET ligand, we selected compounds **6a–c** for radiolabeling and subsequently compound **6b** for the first evaluation in adult C57Bl/6 mice. Besides the high CCR2 receptor affinity and high selectivity over CCR5 and other biological targets, compounds **6a–c** offered the ability to be labeled in an one step nucleophilic substitution ($\text{S}_{\text{N}}2$ -type) reaction of the tosyloxy moiety of **5a–c** with $[\text{}^{18}\text{F}]\text{fluoride}$. Ligands $[\text{}^{18}\text{F}]\text{6a–c}$ were prepared by direct nucleophilic replacement of the tosyloxy moiety with $[\text{}^{18}\text{F}]\text{fluoride}$ in a lead-

Table 2. Off-target affinities/activities of fluorinated ligands **6a–c**.

Cmpd.	$\sigma_1 K_{\text{i}} [\mu\text{M}]$	$\sigma_2 K_{\text{i}} [\mu\text{M}]$	$\alpha_{2A} K_{\text{i}} [\mu\text{M}]$	$\alpha_{2B} K_{\text{i}} [\mu\text{M}]$	M ₃ $K_{\text{i}} [\mu\text{M}]$	5-HT _{2C} $K_{\text{i}} [\mu\text{M}]$	5-HT _{5A} $K_{\text{i}} [\mu\text{M}]$	hERG EC ₅₀ [μM]
6a	1.0	0.74	–	1.2	–	1.02	5.01	2.29 ± 0.31
6b	0.32	7% ^[a]	–	6.81	–	–	–	1.72 ± 0.092
6c	14% ^[a]	17% ^[a]	6.27	–	5.22	–	–	0.671 ± 0.220

Assays: K_{i} values ± SEM from three independent experiments. [a] % inhibition at a test compound's concentration of 10 μM . Radioligands used for receptor binding studies were as follows: σ_1 : $[\text{}^3\text{H}]\text{-}(+)\text{-pentazocine}$, σ_2 : $[\text{}^3\text{H}]\text{ditolylguanidine}$, α_{2A} and α_{2B} : $[\text{}^3\text{H}]\text{rauwolscine}$, M₃: $[\text{}^3\text{H}]\text{QNB}$, 5-HT_{2C}: $[\text{}^3\text{H}]\text{mesulergine}$, 5-HT_{5A}: $[\text{}^3\text{H}]\text{LSD}$, functional assays: FluxOR assay hERG: cisapride.

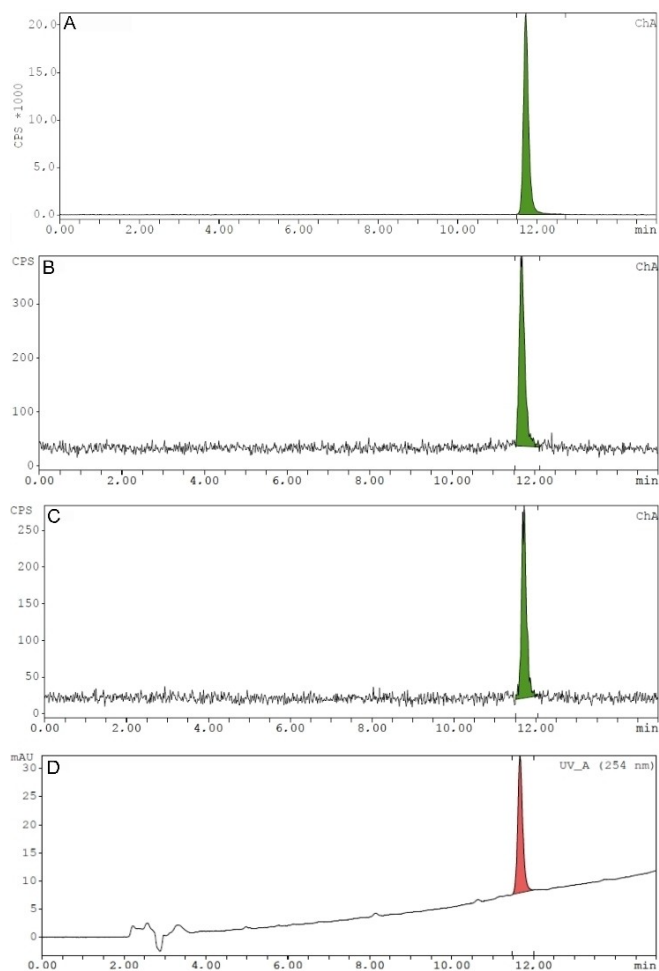


Figure 2. Radio-HPLC chromatograms of A) a typical quality control (QC) of a produced [^{18}F]6b batch and of the *in vitro* stability of [^{18}F]6b after incubation in mouse blood serum at 37 °C after B) 10 min or C) 90 min and D) HPLC chromatogram (UV channel, $\lambda = 254$ nm) of non-radioactive counterpart 6b, measured at analytical HPLC-system B, method B.

shielded computer-controlled TRACERLab Fx_{FDG} radiosynthesizer. In trial experiments, reaction of 5b with [^{18}F]fluoride in DMSO gave a higher radiochemical yield (RCY) of [^{18}F]6b (30%) than in acetonitrile (5.5%). Compounds [^{18}F]6a–c were purified by semipreparative reversed-phase radio-HPLC in high radiochemical purities (>99%). No residual precursors 5a–c or other chemical impurities were detected in the formulated radioligand solution by analytical radio-HPLC. The molar activity (A_m) of the radioligands, when finally formulated for intravenous injection, the RCY and the synthesis times are given in Table 3. Furthermore, the partition coefficient $\log D$ was experimentally determined for the radiolabeled compounds [^{18}F]6a–c at pH of 7.4. Compound [^{18}F]6b is the most lipophilic derivative of the series with a $\log D$ (exp.) of 1.94 ± 0.26 ($n=5$, calculated $\log D$ value, $c\log D$, of 7.00, was calculated by ACD/Chemsketch version ACD/Labs 6.00). For [^{18}F]6a a $\log D$ (exp.) of 1.63 ± 0.17 ($n=5$, $c\log D=6.17$) and for [^{18}F]6c a $\log D$ (exp.) of 1.69 ± 0.16 ($n=5$, $c\log D=8.06$) was determined. An *in vitro* stability study was carried out for all three radiolabeled compounds [^{18}F]6a–c

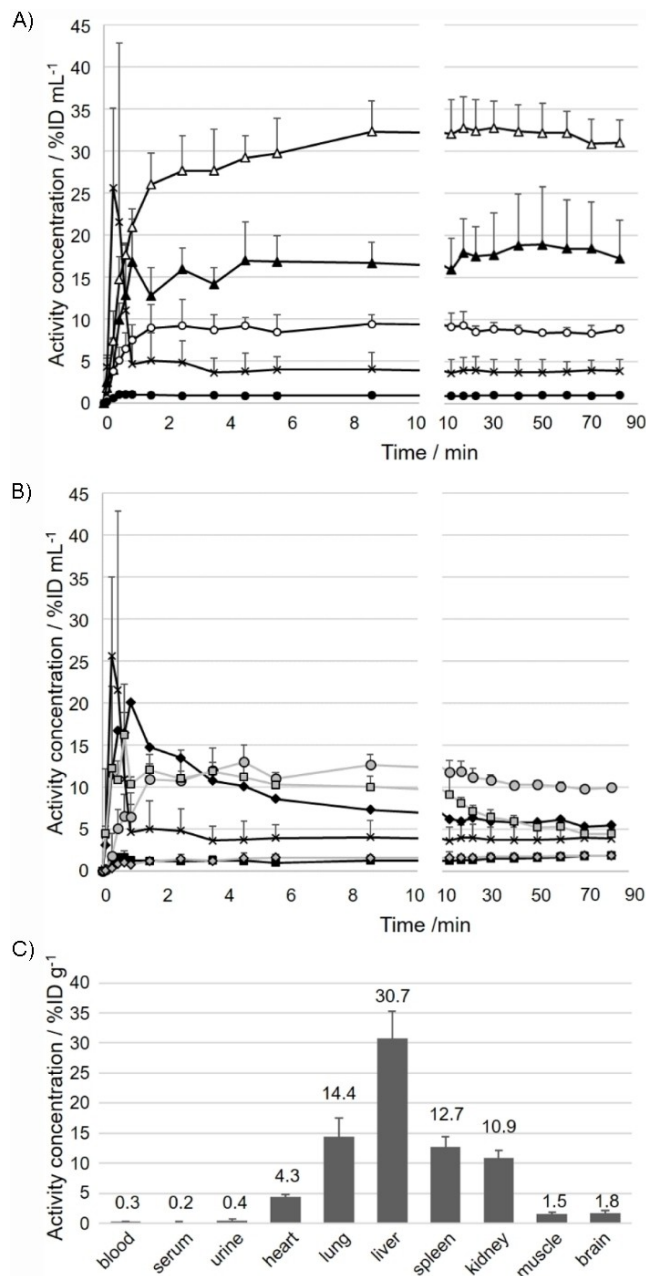


Figure 3. Quantitative analysis of radioactivity distribution in adult C57Bl/6 ($n=6$) after intravenous injection of [^{18}F]6b. In vivo time–activity concentration curves a) and b) illustrate tracer distribution over time in blood (x), liver (Δ), gallbladder (\blacktriangle), kidney (o), bladder (\bullet), brain (\oplus), lung (\blacklozenge), spleen (\ominus), myocardium (\oplus), and muscle (\oplus). In vivo data was complemented by subsequent ex vivo gamma counter analysis c). Results are expressed as mean + S.D. %ID is the percentage of injected dose.

using mouse and human blood serum. During incubation for up to 90 min at 37 °C [^{18}F]6a, [^{18}F]6b and [^{18}F]6c possessed a high stability in both sera. Figure 2 shows exemplarily the data of [^{18}F]6b in mouse blood serum. Only the parent compound [^{18}F]6b was detected by radio-HPLC and no significant radio-metabolites or decomposition products could be observed. The behavior of [^{18}F]6a and [^{18}F]6c is the same (data not shown). Due to its high potency and binding affinity to the CCR2

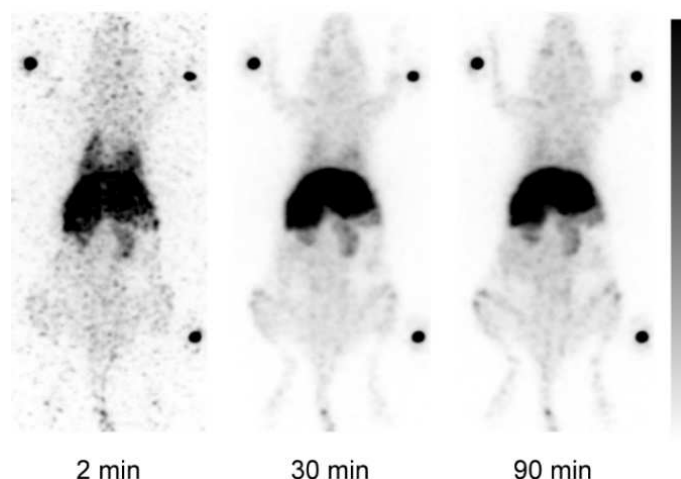


Figure 4. Representative PET image data (maximum intensity projections, ventral view) of the *in vivo* biodistribution of [^{18}F]6b after intravenous injection in an adult female C57Bl/6 mouse.

receptor and its favorable off-target selectivity profile, the fluoropentyl derivative [^{18}F]6b was selected for the biodistribution studies.

Biodistribution of [^{18}F]6b in healthy adult C57Bl/6 mice

The radioactivity distribution of [^{18}F]6b was measured in adult C57Bl/6 mice *in vivo* over 90 minutes by PET/CT. PET images reveal fast and significant accumulation of radioactivity in the liver already in the first minutes after tracer injection that persists until the end of the study (Figure 4). A few minutes post-injection intermediate radioactivity levels were found in the lung, the spleen and the kidneys. Over the course of 90 minutes, the radioactivity concentration in the lungs decreased while the signal in the spleen and the kidneys remained at the same level. Image data do not show the elimination of the tracer and/or its metabolites in the urine. We observed a very slow and only marginally increase of radioactivity in the bones as a sensitive indicator of *in vivo* defluorination of the [^{18}F] labeled tracer, which demonstrated the expected stability of the fluoropentyl group against *in vivo* defluorination. Quantitative analysis by *in vivo* time–activity concentration curves and *ex vivo* gamma counting confirmed the visual impressions (Figure 3). The highly CCR2 selective radioligand [^{18}F]6b demonstrated favorable properties as a new diagnostic tool for PET to elucidate the changes in the distribution and density of CCR2 receptors, revealing their role in the development and pathobiology of inflammation or cancer.

Conclusion

Previously uncovered structure–activity/affinity relationships at CCR2 and CCR5 led the way to the development of highly potent and selective CCR2 receptor antagonists 4a–c and 6a–c, which were further converted into potential ^{18}F -labeled PET

tracer [^{18}F]6a–c. Compounds 6a–c were extensively evaluated for their CCR2 activity/affinity and their off-target selectivity profile at CCR5 receptors and 47 other biological targets (GPCR, ion channels, transporters). The radiolabeled derivatives [^{18}F]6a–c were prepared in high purity (>99%) and high RCY (40–25%). Their $\log D$, murine and human serum plasma stability was determined. The most potent and selective candidate [^{18}F]6b was evaluated *in vivo* in a biodistribution study. Thus displaying a promising profile for further preclinical development.

Experimental Section

Complete protocols for both chemical syntheses and biological methods together with characterization data are presented in the Supporting Information.

Author Contributions

The manuscript was written through the contributions of all authors. All authors have given approval to the final version of the manuscript. A.J. planned and synthesized all compounds. F.M.G. synthesized the precursor 5b in large scale. S.W., A.J. and D.G.S. performed the radiolabeling. Biological assays were performed by D.S., L.H., N.V.O.Z., A.Z., M.M., N.T., M.K. and C.W. The imaging experiments were performed by S.H.

Acknowledgements

K_i determinations and hERG data were generously provided by the National Institute of Mental Health's Psychoactive Drug Screening Program, Contract no. HHSN-271-2018-00023-C (NIMH PDSP). The NIMH PDSP is Directed by Bryan L. Roth MD, PhD at the University of North Carolina at Chapel Hill and Project Officer Jamie Driscoll at NIMH, Bethesda MD, USA. This work was supported by the

Interdisciplinary Center of Clinical Research (IZKF core unit PIX). We would like to thank Christine Bätza, Steffi Bouma, Sarah Köster, Roman Priebe, and Dirk Reinhardt for excellent technical assistance. F.M.G. thanks for the financial support the Brazilian Doctoral Scholarship Program in Federal Republic of Germany: grant no. 290265/2017-7, Conselho Nacional de Desenvolvimento Científico e Tecnológico (CNPq). We are grateful to Fundação de Amparo à Pesquisa do Estado de São Paulo (FAPESP), Coordenação de Aperfeiçoamento de Pessoal de Nível Superior–Brasil (CAPES)–Finance Code 001 and Conselho Nacional de Desenvolvimento Científico e Tecnológico (CNPq) for fundings [grants no. 88881.170193/2018-01 (DGS) and 2017/22001-0 (DGS)]. Open access funding enabled and organized by Projekt DEAL.

Conflict of Interest

The authors declare no conflict of interest.

Keywords: CCR2 · CCR5 antagonists · chemokine receptors · molecular imaging · PET · radiolabeling · TAK-779

- [1] a) G. Bajpai, A. Bredemeyer, W. Li, K. Zaitsev, L. Koenig Andrew, I. Lokshina, J. Mohan, B. Ivey, H.-M. Hsiao, C. Weinheimer, A. Kovacs, S. Epelman, M. Artyomov, D. Kreisel, J. Lavine Kory, *Circulation Res.* **2019**, *124*, 263–278; b) S. Bose, J. Cho, *Arch. Pharm. Res.* **2013**, *36*, 1039–1050.
- [2] M. Ferial, F. Díaz-González, *Expert Opin. Ther. Pat.* **2006**, *16*, 49–57.
- [3] Y. Liu, S. P. Gunsten, D. H. Sultan, H. P. Luehmann, Y. Zhao, T. S. Blackwell, Z. Bollermann-Nowlis, J.-H. Pan, D. E. Byers, J. J. Atkinson, D. Kreisel, M. J. Holtzman, R. J. Gropler, C. Combadiere, S. L. Brody, *Radiology* **2017**, *283*, 758–768.
- [4] G. S. Heo, B. Kopecky, D. Sultan, G. Feng, G. Bajpai, X. Zhang, H. Luehmann, L. Detering, K. Lavine, Y. Liu, *J. Nucl. Med.* **2019**, *60*, 98.
- [5] T. A. Berkhout, H. M. Sarau, K. Moores, J. R. White, N. Elshourbagy, E. Appelbaum, R. J. Reape, M. Brawner, J. Makwana, J. J. Foley, D. B. Schmidt, C. Imburgia, D. McNulty, J. Matthews, K. O'Donnell, D. O'Shannessy, M. Scott, P. H. Groot, C. Macphee, *J. Biol. Chem.* **1997**, *272*, 16404–16413.
- [6] a) C. Combadiere, S. K. Ahuja, H. L. Tiffany, P. M. Murphy, *J. Leukocyte Biol.* **1996**, *60*, 147–152; b) M. Samson, O. Labbe, C. Mollereau, G. Vassart, M. Parmentier, *Biochemistry* **1996**, *35*, 3362–3367.
- [7] L. Fantuzzi, M. Tagliamonte, M. C. Gauzzi, L. Lopalco, *Cell. Mol. Life Sci.* **2019**, *76*, 4869–4886.
- [8] a) A. Junker, A. K. Kokornaczyk, A. J. M. Zweemer, B. Frehland, D. Schepmann, J. Yamaguchi, K. Itami, A. Faust, S. Hermann, S. Wagner, M. Schafers, M. Koch, C. Weiss, L. H. Heitman, K. Kopka, B. Wunsch, *Org. Biomol. Chem.* **2015**, *13*, 2407–2422; b) A. K. Strunz, A. J. M. Zweemer, C. Weiss, D. Schepmann, A. Junker, L. H. Heitman, M. Koch, B. Wunsch, *Bioorg. Med. Chem.* **2015**, *23*, 4034–4049.
- [9] S. Thum, A. K. Kokornaczyk, T. Seki, M. De Maria, N. V. Ortiz Zacarias, H. de Vries, C. Weiss, M. Koch, D. Schepmann, M. Kitamura, N. Tschammer, L. H. Heitman, A. Junker, B. Wunsch, *Eur. J. Med. Chem.* **2017**, *135*, 401–413.
- [10] D. W. Kim, H.-J. Jeong, S. T. Lim, M.-H. Sohn, *Angew. Chem. Int. Ed.* **2008**, *47*, 8404–8406; *Angew. Chem.* **2008**, *120*, 8532–8534.
- [11] M. Bruehlmeier, U. Roelcke, P. A. Schubiger, S. M. Ametamey, *J. Nucl. Med.* **2004**, *45*, 1851–1859.
- [12] P. W. Miller, N. J. Long, R. Vilar, A. D. Gee, *Angew. Chem. Int. Ed.* **2008**, *47*, 8998–9033; *Angew. Chem.* **2008**, *120*, 9136–9172.

Manuscript received: September 16, 2020

Revised manuscript received: November 4, 2020

Accepted manuscript online: November 18, 2020

Version of record online: November 23, 2020